

ORIGINAL ARTICLE

A novel strategy inducing autophagic cell death in Burkitt's lymphoma cells with anti-CD19-targeted liposomal rapamycin

K Ono, T Sato, S Iyama, A Tatekoshi, A Hashimoto, Y Kamihara, H Horiguchi, S Kikuchi, Y Kawano, K Takada, T Hayashi, K Miyanishi, Y Sato, R Takimoto, M Kobune and J Kato

Relapsed or refractory Burkitt's lymphoma often has a poor prognosis in spite of intensive chemotherapy that induces apoptotic and/or necrotic death of lymphoma cells. Rapamycin (Rap) brings about autophagy, and could be another treatment. Further, anti-CD19-targeted liposomal delivery may enable Rap to kill lymphoma cells specifically. Rap was encapsulated by anionic liposome and conjugated with anti-CD19 antibody (CD19-GL-Rap) or anti-CD2 antibody (CD2-GL-Rap) as a control. A fluorescent probe Cy5.5 was also liposomized in the same way (CD19 or CD2-GL-Cy5.5) to examine the efficacy of anti-CD19-targeted liposomal delivery into CD19-positive Burkitt's lymphoma cell line, SKW6.4. CD19-GL-Cy5.5 was more effectively uptaken into SKW6.4 cells than CD2-GL-Cy5.5 *in vitro*. When the cells were inoculated subcutaneously into nonobese diabetic/severe combined immunodeficiency mice, intravenously administered CD19-GL-Cy5.5 made the subcutaneous tumor fluorescent, while CD2-GL-Cy5.5 did not. Further, CD19-GL-Rap had a greater cytotoxic effect on not only SKW6.4 cells but also Burkitt's lymphoma cells derived from patients than CD2-GL-Rap *in vitro*. The specific toxicity of CD19-GL-Rap was cancelled by neutralizing anti-CD19 antibody. The survival period of mice treated with intravenous CD19-GL-Rap was significantly longer than that of mice treated with CD2-GL-Rap after intraperitoneal inoculation of SKW6.4 cells. Anti-CD19-targeted liposomal Rap could be a promising lymphoma cell-specific treatment inducing autophagic cell death.

Blood Cancer Journal (2014) 4, e180; doi:10.1038/bcj.2014.2; published online 7 February 2014

Keywords: CD19; liposome; rapamycin; Burkitt's lymphoma

INTRODUCTION

Burkitt's lymphoma is a highly aggressive B-cell non-Hodgkin lymphoma. The outcome of intensive chemotherapy has improved and is now excellent in children, but the prognosis is still poor in elderly adults.¹

To obtain a better outcome, there are at least two challenges. One is the introduction of molecular targeted drugs. The mammalian target of rapamycin (mTOR) inhibitor, rapamycin (Rap), is one of the plausible candidates as the drug significantly decreased tumor growth, splenomegaly and metastasis to bone marrow in mice transplanted with Burkitt's lymphoma cells.^{2,3} Further, Rap induces autophagic cell death in cancer cells;⁴ this signal transduction is independent of the apoptotic or necrotic pathway and functions as a backup if apoptosis or necrosis is blocked.⁵ This indicates that Rap is still a hopeful drug even when conventional chemotherapeutic reagents are not fully effective.

The other approach is the application of a specific drug delivery system. It is quite reasonable to select CD19 to target Burkitt's lymphoma cells as they highly express CD19 on their surface.⁶ In addition, there are no 'theoretical' limitations to the concomitant use of chimeric monoclonal antibody against CD20, rituximab. In previous reports, to target human B-cell malignancies, anti-CD19-targeted liposomal doxorubicin or imatinib was successfully prepared against lymphoma cells^{7,8} or acute lymphoblastic leukemia cells,⁹ respectively, with the use of stealth immunoliposome technique, by which antibodies are conjugated to polyethylene glycol (PEG) in liposome, that is,

PEG-immunoliposome. Although the anti-CD19-targeted PEG-immunoliposomal doxorubicin elongated the survival period of mouse xenograft model bearing lymphoma cells, specific accumulation into lymphoma cells with no uptake by spleen or liver of their anti-CD19-targeted PEG-immunoliposome was not demonstrated *in vivo*.^{7,8}

In order to reduce the nonspecific uptake of liposome by macrophages in the reticuloendothelial system, anionic (negatively charged) liposome is preferable to cationic (positively charged) one, which is often used to encapsulate negatively charged DNA by electrostatic interaction. This is because cationic liposomes tend to aggregate in the presence of serum and to be associated with serum protein: these characters may lead to the high uptake of cationic liposomes by reticuloendothelial system.¹⁰

We recently demonstrated that anionic liposome bound to L-fucose enabled strict delivery to pancreatic cancer tumor without uptake of liposome by the spleen or liver *in vivo*.¹¹ With the use of this technology, in this study, we prepared anti-CD19-targeted anionic liposomal Rap for Burkitt's lymphoma and evaluated its efficacy and safety.

MATERIALS AND METHODS

Cell culture

Three human Burkitt's lymphoma cell lines, SKW6.4, Raji and Namalwa cells, were supplied by American Type Culture Collection (Manassas, VA, USA) and maintained in RPMI 1640 (Gibco BRL, Tokyo, Japan) with 10% heat-inactivated fetal bovine serum (Sigma, St Louis, MO, USA).

The doxorubicin-resistant SKW6.4 subline, designated SKW-DOX, was obtained by continuous exposure of SKW6.4 cells to 10 ng/ml of doxorubicin for >70 passages. To obtain SKW6.4 cells with red fluorescence, which can be detected *in vivo* by IVIS Imaging System (Caliper Life Science, Hopkinton, MA, USA), the cells were transduced with red-fluorescent protein (RFP) gene by using expression lentiviral particles, pre-made lentivirus for RFP (GenTarget, San Diego, CA, USA). After transfection according to the manufacturer's instructions, red-fluorescent cells were further selected by flow cytometry on a FACSAria cell sorter (BD Biosciences, San Diego, CA, USA). The red-fluorescent SKW6.4 subline was designated SKW-RFP.

Lymphoma cells from patients

Lymphoma cells were obtained from two patients with Burkitt's lymphoma after informed consent was obtained in accordance with the Declaration of Helsinki and institutional ethics committee approval from the Sapporo Medical University Human Ethics Committee. One sample was collected from pleural effusion and the other from peripheral blood that was collected when the patient was in the leukemic phase. Lymphoma cells were positively selected with the use of anti-CD19-coated magnetic beads (Dynabeads M-450 Pan B; Dynal, Oslo, Norway) according to the manufacturer's instructions.

Reagents

Rap and Benzoyloxycarbonyl-Val-Ala-Asp (OMe) fluoromethylketone (Z-VAD-FMK) were purchased from Medical and Biological Laboratories (MBL, Nagoya, Japan). *N*-acetyl-L-cysteine and 3-methyladenine were purchased from Wako Pure Chemical Industries (Osaka, Japan). Doxorubicin was purchased from Sigma.

Preparation of liposome

Preparation of hydrophilic anionic liposomes and encapsulation of Cy5.5 or Rap were carried out as described previously.^{11–13} These liposomes (GLYCOLIPO, Katayama Chemical Industries, Osaka, Japan) were composed of dipalmitoylphosphatidylcholine, dipalmitoylphosphatidylethanolamine, dicetylphosphate, cholesterol and ganglioside. Dicetylphosphate was used to confer a negative charge to the liposome surface. Briefly, dipalmitoylphosphatidylcholine, cholesterol, ganglioside dicetylphosphate and dipalmitoylphosphatidylethanolamine were mixed at different molar ratios and cholic acid was added to facilitate micelle formation. The mixture was dissolved in methanol/chloroform (1:1, v/v) and the solvent evaporated at 37 °C to produce a lipid film, which was dried under vacuum. This was then dissolved in 10 mM TAPS buffer (*N*-tris(hydroxymethyl)methyl-3-amino-propane sulfonic acid containing buffer) without NaCl at pH 8.4, and sonicated to obtain a suspension of uniform micelles. Cy5.5, or Rap solution was then added to the micelle suspension, which was then ultrafiltered (molecular cutoff 10 000) (Amicon PM10, Millipore, Billerica, MA, USA). Tris(hydroxymethyl)aminomethane (Tris) was crosslinked on the liposome surface via bis(sulfosuccinimidyl)suberate (BS3) to confer hydrophilicity. Using 3,30-dithiobis(sulfosuccinimidyl)propionate, anti-CD19 monoclonal antibody (clone J3-119, Beckman Coulter, Villepinte, France) or anti-CD2 monoclonal antibody (clone 39C1.5, Beckman Coulter) was crosslinked to human serum albumin, which was coupled in advance to the ganglioside component of liposomes. Anti-CD19 or CD2 antibody was added to a final concentration of 75 µg/ml and stirred at 25 °C for 2 h. Tris-HCl was then added to reach a final concentration of 132 mg/ml, and stirred overnight at 4 °C for hydrophilization of the liposome surface. The content of lipid in liposomes was determined as total cholesterol in the presence of 0.5% TritonX-100 with a Determiner TC555 diagnostic kit (Kyowa Medex, Tokyo, Japan). The particle size and zeta-potential were measured using Zetasizer Nano-S90 (Malvern Instruments, Worcestershire, UK). The amount of anti-CD19 or CD2 antibody on the surface of liposomes was measured by enzyme-linked immunosorbent assay using CD19 or CD2-immobilized microplate as described previously.¹³ The concentration of Rap in liposomes was determined by high-performance liquid chromatography assay with ultraviolet detection as described previously.¹⁴ For electron microscopic analysis, a Hitachi H-7000 electron microscope (Hitachi, Japan) was used. The uptake of Cy5.5-encapsulating liposome *in vitro* was detected fluorescence microscopically using Biozero BZ-8100 (Keyence, Osaka, Japan) and flow cytometrically using FACSCanto flow cytometer (BD Biosciences).

In vitro cell proliferation assay

In all, 0.5×10^5 cells seeded onto a 96-well culture plate were stimulated with liposomal Rap and cultured for 72 h. The number of viable cells was quantified using Premix WST-1 Cell Proliferation Assay System (TaKaRa, Kyoto, Japan) according to the manufacturer's instructions. Briefly, 10 µl of Premix WST-1 per 100 µl of culture medium was added to each well and the cells were incubated under the standard culture condition for 1 h. WST reduction was determined with an automated enzyme-linked immunosorbent assay plate reader, ImmunonMini NJ-2300 spectrophotometer (InterMed, Tokyo, Japan), at an optical density of 450–650 nm.

Western blotting

In all, 1×10^6 cells were lysed in a buffer containing 1% sodium dodecyl sulfate, 20 mM Tris-HCl pH 7.4, 5 µg/ml pepstatin A, 10 µg/ml leupeptin, 5 µg/ml aprotinin and 1 mM phenyl-methylsulfonyl fluoride and then boiled for 5 min. After passage through a 20-gauge needle 10 times and centrifugation at 15 000 r.p.m. at 4 °C for 30 min, the aliquot was boiled in a standard reducing sample buffer for 3 min and subjected to sodium dodecyl sulfate-polyacrylamide gel electrophoresis. It was followed by transfer to Immobilon-P membrane (Millipore, Bedford, MA, USA) and hybridization with rabbit anti-LC3B (D11) XP (Cell Signaling, Beverly, MA, USA). Proteins were visualized by enhanced chemiluminescence (Amersham Pharmacia Biotech, Uppsala, Sweden).

Animals

Nonobese diabetic/severe combined immunodeficiency (NOD/SCID) female mice of 6–7 weeks of age and weighing 19–21 g were obtained from Charles River Laboratories (Yokohama, Japan). The mice were kept under specific pathogen-free conditions with a 12-h light:12-h dark cycle and free access to food and water, and received humane care in compliance with Institutional Guidelines. All experiments were approved by the Animal Care and Use Committee of Sapporo Medical University.

In order to examine the specific delivery of anti-CD19-targeted liposome, 1.0×10^7 SKW6.4 cells were inoculated subcutaneously on the left side of the back of NOD/SCID mice. Seven days after the inoculation, 100 µl of anti-CD19 or CD2-targeted liposomal Cy5.5 was administered once via the tail vein. The red fluorescence of Cy5.5 uptaken in the tumor was detected by IVIS Imaging System, IVIS Lumina II with Living Image software version 3.0 (Caliper Life Science).

For confirmation of transplantability and preliminary examination of *in vivo* distribution, 2.0×10^6 SKW-RFP cells were intraperitoneally inoculated into NOD/SCID mice. Thirty days after inoculation, red fluorescence in the lymph nodes was detected extracorporeally and laparotomically by the IVIS Imaging System. The expression of CD19 on SKW-RFP cells in lymph nodes was detected by immunohistochemical staining using the standard protocol.

To examine the specific antitumor effects of anti-CD19-targeted liposomal Rap, 2.0×10^6 SKW-RFP cells were intraperitoneally inoculated into NOD/SCID mice. Then, anti-CD19 or CD2-targeted liposome containing 30 µg of Rap was administered via the tail vein twice weekly. The mice were checked daily for survival. Red fluorescence of the lymph nodes was estimated extracorporeally by the IVIS photon-counting system once weekly.

Statistical analysis

All statistical analyses were performed using GraphPad Prism version 5.0 (GraphPad Software, La Jolla, CA, USA). Statistical analyses of paired data were performed by Student's *t*-test for the *in vitro* assays, while log-rank test was used to analyze statistical significance for *in vivo* survival curves constructed using the Kaplan–Meier method. Statistical significance was defined as $P < 0.05$.

RESULTS

Specific delivery of anti-CD19-targeted liposome

To evaluate specific delivery of anti-CD19-targeted liposome into CD19-expressing Burkitt's lymphoma cells, a fluorescent dye, Cy5.5, was encapsulated in an anionic liposome, Glycolipo (GL-Cy5.5), which was further conjugated with anti-CD19 antibody (CD19-GL-Cy5.5) or anti-CD2 antibody (CD2-GL-Cy5.5) as a negative control. Among three CD19-expressing Burkitt's

lymphoma cell lines, SKW6.4, Raji and Namalwa cells, SKW6.4 cells were selected for further experiments because the cells were most susceptible to Rap (Supplementary Figure S1). When SKW6.4 cells were exposed to Glycolipo (GL), GL-Cy5.5 or CD2-GL-Cy5.5, the mean fluorescence intensity value was 123, 372 or 391 in flow cytometric analysis, respectively; meanwhile, it was 1891 when the cells were treated by CD19-GL-Cy5.5 (Figure 1b). The fluorescence microscopic images were also presented (Figure 1a). Next, SKW6.4 cells were inoculated subcutaneously on the left side of the back of NOD/SCID mice. The accumulation of CD19-GL-Cy5.5 in the subcutaneous tumor could be detected by the IVIS Imaging System 1 day after it was injected via the tail vein.

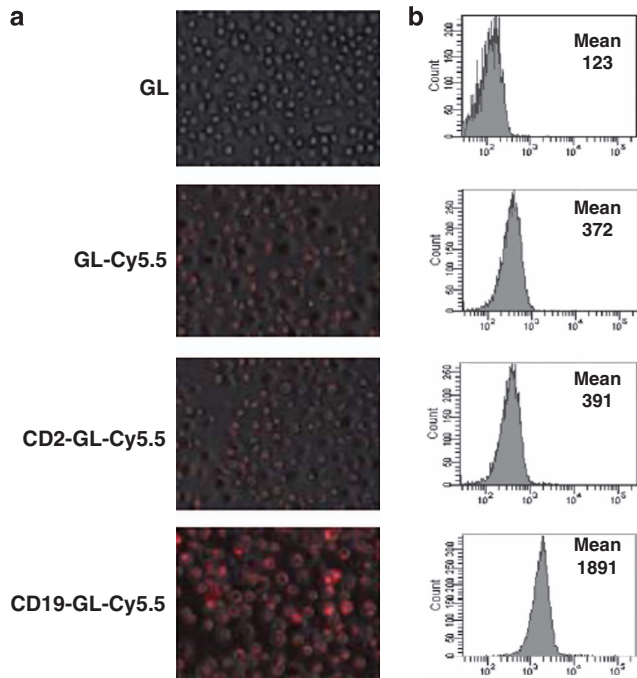


Figure 1. Specificity of anti-CD19-targeted liposome against SKW6.4 cells *in vitro*. In all, 1.0×10^6 SKW6.4 cells were cultured with 50 μ l of GL, GL-Cy5.5, CD2-GL-Cy5.5 or CD19-GL-Cy5.5 for 24 h. Representative fluorescence microscopic images (a) and histograms of flow cytometry (b) are shown. Mean channel fluorescence is shown in each histogram.

The fluorescence of the tumor on day 2 was the brightest, and gradually decreased thereafter. On the other hand, fluorescence was not detected at any time in the tumor of mice that had been injected with CD2-GL-Cy5.5 (Figure 2). The nonspecific uptake by spleen and liver was not negligible when mice were observed in ventral view with longer exposure time (data not shown); however, the specific uptake by tumor was easily detected without nonspecific fluorescence of liver and spleen in dorsal view.

Preparation of anti-CD19-targeted liposomal Rap

Rap was encapsulated in GL (GL-Rap), which was then conjugated with anti-CD19 antibody (CD19-GL-Rap) or anti-CD2 antibody (CD2-GL-Rap). GL, GL-Rap, CD2-GL-Rap and CD19-GL-Rap were all spherical in shape as demonstrated by transmission electron microscopy and uniform in size distribution as demonstrated by Zetasizer Nano-S90 (Figure 3). Reasonably, the vacant liposome, GL, was smaller than GL containing Rap, that is, GL-Rap, CD2-GL-Rap and CD19-GL-Rap (Figure 3). The mean particle sizes, lipid concentrations, zeta potentials, Rap concentrations and antibody concentrations of GL, GL-Rap, CD2-GL-Rap or CD19-GL-Rap are shown in Table 1.

Cytocidal activity of anti-CD19-targeted liposomal Rap *in vitro*

The cytotoxic effects of CD19-GL-Rap on SKW6.4 cells were examined as shown in Figures 4a and b. The cytotoxic effects were examined using WST-1 cell proliferation assay. CD19-GL-Rap containing 1 nM of Rap induced 66% cell death, while GL-Rap or CD2-GL-Rap containing the same dosage of Rap induced 13% or 11% cell death, respectively. When CD19-GL-Rap containing a higher concentration of Rap of 10 nM was administered, 89% cell death was induced (Figure 4a). The cell death induced by CD19-GL-Rap was inhibited by a neutralizing anti-CD19 antibody in a dose-dependent manner. On the other hand, a neutralizing anti-CD2 antibody could not reproduce the inhibiting effect by anti-CD19 antibody (Figure 4b). Then, samples from two patients with Burkitt's lymphoma were examined. One sample was collected from pleural effusion and the other was a peripheral blood sample that had been collected when the patient was in the leukemic phase. Magnetic beads were used for selection of CD19-positive cells. Both samples were readily susceptible: CD19-GL-Rap containing 10 nM Rap induced 85% or 97% cell death, respectively (Figure 4c).

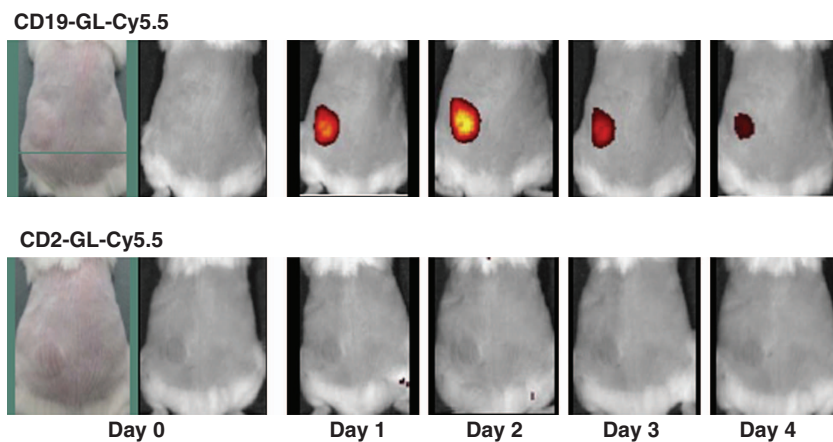


Figure 2. Specificity of anti-CD19-targeted liposome against SKW6.4 cells *in vivo*. In all, 1.0×10^7 SKW6.4 cells were subcutaneously inoculated into NOD/SCID mice. Seven days after inoculation, 100 μ l of CD19-GL-Cy5.5 or CD2-GL-Cy5.5 was administered once via the tail vein. Red fluorescence of Cy5.5 uptaken in the tumor was detected by IVIS Imaging System. This experiment was repeated and confirmed.

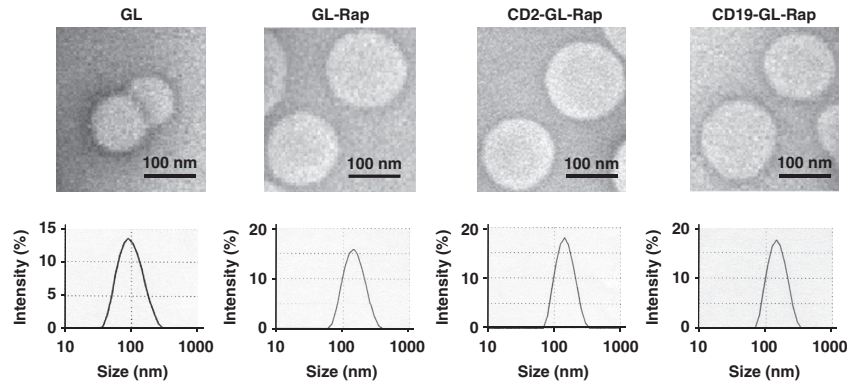


Figure 3. Characteristics of anti-CD19-targeted liposomal Rap. Representative transmission electron microscopic images and size distributions of GL, GL-Rap, CD2-GL-Rap and CD19-GL-Rap are shown.

Table 1. Physicochemical characteristics of anti-CD19-targeted liposomal Rap				
	GL	GL-Rap	CD2-GL-Rap	CD19-GL-Rap
Particle size (nm)	93	139	139	140
Lipid concentration (mg/ml)	32	30	31	30
Zeta potential (mV)	-64	-66	-66	-65
Rap concentration (mg/ml)	0	1.2	1.3	1.2
Antibody concentration ($\mu\text{g/ml}$)	0	0	128	121

Abbreviations: GL, Glycolipo; Rap, rapamycin.

Autophagic cell death-inducing activity of anti-CD19-targeted liposomal Rap

The cell death of SKW6.4 induced by CD19-GL-Rap was proven to be autophagic by western blot analysis of LC3, in which Rap increased the level of the autophagosomal marker, LC3-II, in a dose-dependent manner (Figure 5a). Further confirmation was obtained by experiments using an autophagy inhibitor, 3-methyladenine. 3-Methyladenine effectively suppressed the cell death of SKW6.4 induced by CD19-GL-Rap (Figure 5b). Neither a pan-caspase inhibitor, Benzoyloxycarbonyl-Val-Ala-Asp (OMe) fluoromethylketone (Z-VAD-FMK) (Figure 5c) nor the reactive oxygen species scavenger, *N*-acetyl-L-cysteine (Figure 5d), inhibited the cytotoxic effects of CD19-GL-Rap, indicating that the cell death of SKW6.4 induced by CD19-GL-Rap was not apoptotic nor necrotic.

Cell death induced by anti-CD19-targeted liposomal Rap in doxorubicin-resistant cells

Next, we prepared a doxorubicin-resistant subline of SKW6.4 cells named SKW-DOX by long-time exposure of parental SKW6.4 cells to low-dose doxorubicin in order to examine whether the autophagy-inducing effect of CD19-GL-Rap was still effective even when SKW6.4 cells have acquired resistance to a representative chemotherapeutic agent for lymphoma, doxorubicin. As shown in Supplementary Figure S2A, SKW-DOX cells were resistant to doxorubicin with 77% of the cells surviving when incubated with 100 ng/ml of doxorubicin, while only 10% of parental SKW6.4 cells survived when incubated with the same dosage. Nevertheless, SKW-DOX cells were still sensitive to the autophagy-inducing effect of CD19-GL-Rap as much as the parental SKW6.4 cells (Supplementary Figure S2B).

Antitumor activity of anti-CD19-targeted liposomal Rap *in vivo*

For *in vivo* experiments, red-fluorescent SKW6.4 cells named SKW-RFP were prepared by lentiviral gene transfection of RFP into

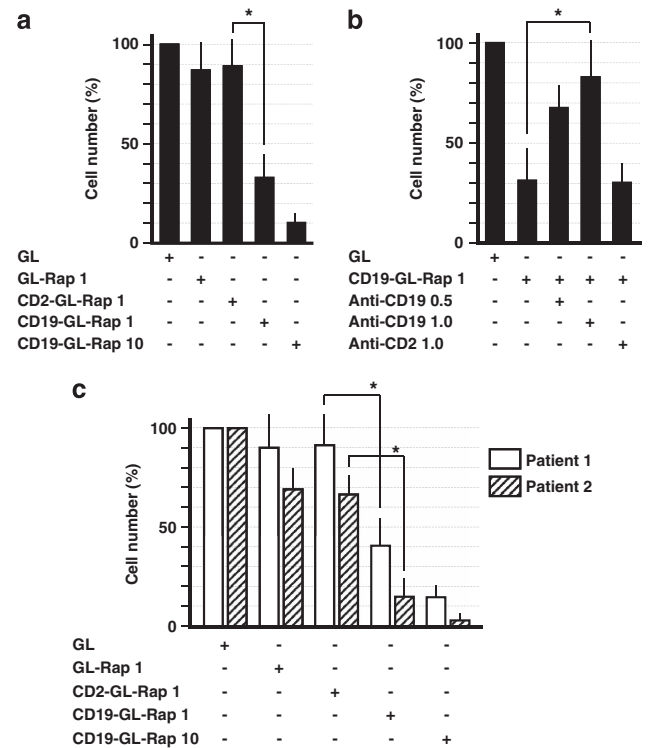


Figure 4. Cytotoxic effects of anti-CD19-targeted liposomal Rap against SKW6.4 cells and Burkitt's lymphoma cells from patients. (a) In all, 0.5×10^5 SKW6.4 cells were cultured with GL-Rap, CD2-GL-Rap or CD19-GL-Rap containing 1 or 10 nM Rap for 72 h. (b) In total, 0.5×10^5 SKW6.4 cells were cultured with CD19-GL-Rap containing 1 nM Rap for 72 h that had been pretreated with anti-CD19 antibody (0.5 or 1.0 $\mu\text{g/ml}$) or anti-CD2 antibody (1.0 $\mu\text{g/ml}$). (c) In all, 0.5×10^5 Burkitt's lymphoma cells from patients were cultured with GL-Rap, CD2-GL-Rap or CD19-GL-Rap containing 1 or 10 nM Rap for 72 h. Cell number was estimated using WST-1 reagent ($n = 6$). $*P < 0.01$.

the parental SKW6.4 cells. When SKW-RFP cells were inoculated into NOD/SCID mice intraperitoneally, mesenteric and retroperitoneal lymph nodes became extremely swollen, of which red fluorescence was easily detected by IVIS both extracorporeally and laparotomically (Supplementary Figure S3A). Immunohistochemical staining of lymph nodes confirmed the expression of CD19 on SKW-RFP cells (Supplementary Figure S3B).

After intraperitoneal inoculation of SKW-RFP cells, NOD/SCID mice were treated with GL, 30 μg of Rap, GL-Rap, CD2-GL-Rap or

CD19-GL-Rap containing the same dosage of Rap twice weekly. The red fluorescence of abdominal lymph nodes was extracorporeally quantified as 'photons' by IVIS. Photons in mice treated with GL increased rapidly after day 21 while photons in mice treated with Rap, GL-Rap or CD2-GL-Rap did so after day 28. Compared with Rap, GL-Rap or CD2-GL-Rap, CD19-GL-Rap more effectively slowed the increase of photons (Figure 6a). Actually, the number of abdominal photons of mice treated with CD19-GL-Rap was much lower than that of mice treated with Rap, GL-Rap or CD2-GL-Rap on day 35 ($P < 0.01$; Figure 6b).

The antitumor effects of CD19-GL-Rap were also evaluated by survival of mice in the same *in vivo* experiments (Figure 6c). All five mice treated with GL (median survival time (MST) 33 days) died between day 31 and 34 while the mice treated with Rap (MST 36 days), GL-Rap (MST 37 days) or CD2-GL-Rap (MST 40 days) died between day 35 and day 42. Although Rap, GL-Rap or CD2-GL-Rap elongated the survival period of mice as compared with GL ($P < 0.01$), the life-saving effect of CD19-GL-Rap (MST 57 days) exceeded those of Rap, GL-Rap or CD2-GL-Rap ($P < 0.01$).

As for adverse effects of CD19-GL-Rap, there were no abnormal data in complete blood count and blood chemistry after intravenous administration of CD19-GL-Rap containing 30 μg of Rap two times a week into mice (SupplementaryTable S1).

DISCUSSION

As for the target of liposomal drug delivery for B-cell lymphoma, Saprana and Allen¹⁵ stated that not only CD20 but also CD19 was suitable. They have shown that anti-CD19-targeted liposomal doxorubicin as well as anti-CD20-targeted one had therapeutic efficacy against human B-lymphoma cells.

However, it is questionable whether doxorubicin is the best choice as a drug contained in anti-CD19-targeted liposome for incurable types of B-cell lymphoma such as Burkitt's lymphoma in spite of conventional chemotherapies containing doxorubicin. A different type of drug from chemotherapeutic reagents conventionally used should be applied. In this context, we have chosen Rap that induces autophagic cell death and is independent of the apoptotic/necrotic signaling pathway induced by conventional chemotherapeutic reagents such as doxorubicin.¹⁶

Actually, anti-CD19-targeted liposomal Rap, which we have prepared, had specific cytotoxic effects for Burkitt's lymphoma cells even when the cells were resistant to doxorubicin (Supplementary Figure S2). These results might indicate that our strategy could be applicable to relapsed or refractory lymphoma after first-line chemotherapy. In addition, other types of mTOR inhibitor, temsirolimus and everolimus, could be applied in our anti-CD19-targeted liposomal system instead of Rap as these

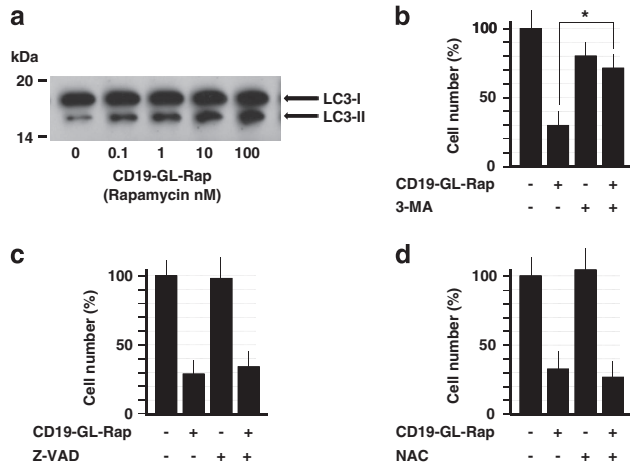


Figure 5. Autophagic cell death-inducing effects of anti-CD19-targeted liposomal Rap. (a) In all, 1.0×10^6 SKW6.4 cells were cultured with CD19-GL-Rap containing 0–100 nM Rap for 6 h. LC3 was detected by western blot analysis. In total, 0.5×10^5 SKW6.4 cells were cultured with CD19-GL-Rap containing 1 nM Rap with or without 10 μM of autophagy inhibitor, 3-methyladenine (b), 40 μM of pan-caspase inhibitor, Z-VAD-FMK (c) or 20 mM of reactive oxygen species scavenger, N-acetyl-L-cysteine (d) for 72 h. Cell number was estimated using WST-1 reagent ($n = 6$). * $P < 0.01$.

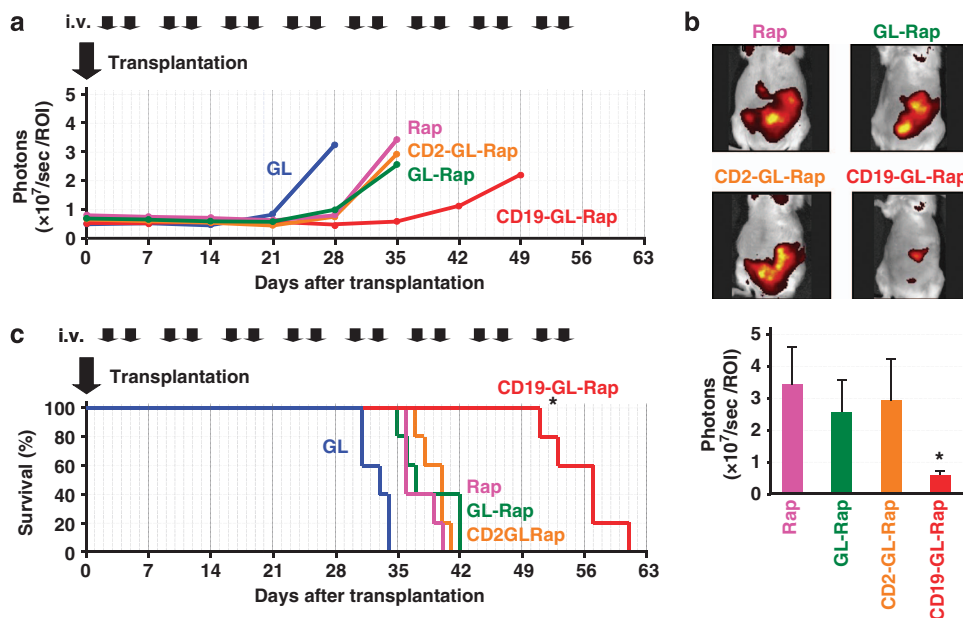


Figure 6. Survival benefits from anti-CD19-targeted liposomal Rap therapy. (a) In all, 2.0×10^6 red-fluorescent SKW-RFP cells were intraperitoneally inoculated into NOD/SCID mice ($n = 5$). GL, 30 μg of Rap or GL-Rap, CD2-GL-Rap, or CD19-GL-Rap containing 30 μg of Rap was administered via the tail vein twice weekly. Red fluorescence estimated extracorporeally by the IVIS Imaging System (photons) is shown. (b) Representative IVIS images and photons on day 35 are shown. * $P < 0.01$ compared with Rap, GL-Rap or CD2-GL-Rap. (c) Survival of mice was demonstrated. This experiment was repeated and confirmed.

mTOR inhibitors also induced cell death effectively in SKW6.4 cells (data not shown).

Apart from its anti-lymphoma activity, there is another merit to selecting Rap for anti-CD19-targeted liposomal system, that is, safety. Rap has been used for immunosuppression in organ allografting. The most common adverse effects are hyperlipidemia and dose-dependent myelosuppression;¹⁷ however, the safety of our strategy for clinical application should be examined carefully.

Concerning the type of liposome, anionic liposome was chosen in our system as we previously succeeded in specific delivery of anticancer drugs into pancreatic cancer cells with the use of fucose-conjugated anionic liposome.¹¹ This technique was applied to encapsulating Rap and conjugation of anti-CD19 antibody in this study. Meanwhile, there was an interesting report concerning the charge of the liposome.¹⁸ Anionic liposomes with PEGylation encapsulating doxorubicin showed significant enhancement of not only *in vitro* uptake and cell inhibition but also *in vivo* tumor inhibition compared with neutral ones. These results might support our choice in this report of not neutral PEG-immunoliposome but anionic liposome conjugated with antibody.

Besides, there have been issues, which should be taken into consideration for the clinical application of our strategy. One is the loss of CD19 expression on Burkitt's lymphoma cells after the exposure to CD19-GL-Rap since that phenomenon was reported when precursor-B acute lymphoblastic leukemia patients were treated with blinatumomab, the antibody engaging CD3-expressing T cells to CD19-expressing B cells.¹⁹ The other is acquired resistance against Rap: resistance emerged quickly via increases in mTORC2 signaling after the Rap administration reduced tumor burden in LMP2A/Myc transgenic mice.²

In conclusion, we have successfully demonstrated that anti-CD19-targeted liposomal Rap induced autophagic cell death specifically in Burkitt's lymphoma cells despite doxorubicin resistance. We consider our strategy as promising for clinical application.

CONFLICT OF INTEREST

The authors declare no conflict of interest.

ACKNOWLEDGEMENTS

This work was supported by Grant-in-Aid for Scientific Research (C:22591043 to TS, MK and JK) from Japan Society for the Promotion of Science.

AUTHOR CONTRIBUTIONS

KO and TS designed and performed the research, analyzed and interpreted the data, and wrote the manuscript; AT, AH, YK, HH and SK analyzed data and performed research; SI, YK and KT analyzed the data and edited the manuscript; TH, KM, YS, RT, MK and JK analyzed the data and edited and approved the final version of the manuscript.

REFERENCES

- Molyneux EM, Rochford R, Griffin B, Newton R, Jackson G, Menon G *et al*. Burkitt's lymphoma. *Lancet* 2012; **379**: 1234–1244.
- Cen O, Longnecker R. Rapamycin reverses splenomegaly and inhibits tumor development in a transgenic model of Epstein-Barr virus-related Burkitt's lymphoma. *Mol Cancer Ther* 2011; **10**: 679–686.
- Nepomuceno RR, Balatoni CE, Natkunam Y, Snow AL, Krams SM, Martinez OM. Rapamycin inhibits the interleukin 10 signal transduction pathway and the growth of Epstein Barr virus B-cell lymphomas. *Cancer Res* 2003; **63**: 4472–4480.
- Easton JB, Houghton PJ. mTOR and cancer therapy. *Oncogene* 2006; **25**: 6436–6446.
- Chaabane W, User SD, El-Gazzah M, Jaksik R, Sajjadi E, Rzeszowska-Wolny J *et al*. Autophagy, apoptosis, mitoptosis and necrosis: interdependence between those pathways and effects on cancer. *Arch Immunol Ther Exp (Warsz)* 2013; **61**: 43–58.
- Perkins AS, Friedberg JW. Burkitt lymphoma in adults. *Hematology Am Soc Hematol Educ Program* 2008; 341–348 (doi:10.1182/asheducation-2008.1.341).
- Sapra P, Moase EH, Ma J, Allen TM. Improved therapeutic responses in a xenograft model of human B lymphoma (Namalwa) for liposomal vincristine versus liposomal doxorubicin targeted via anti-CD19 IgG2a or Fab' fragments. *Clin Cancer Res* 2004; **10**: 1100–1111.
- Allen TM, Mumbengegwi DR, Charrois GJ. Anti-CD19-targeted liposomal doxorubicin improves the therapeutic efficacy in murine B-cell lymphoma and ameliorates the toxicity of liposomes with varying drug release rates. *Clin Cancer Res* 2005; **11**: 3567–3573.
- Harata M, Soda Y, Tani K, Ooi J, Takizawa T, Chen M *et al*. CD19-targeting liposomes containing imatinib efficiently kill Philadelphia chromosome-positive acute lymphoblastic leukemia cells. *Blood* 2004; **104**: 1442–1449.
- Oku N, Tokudome Y, Namba Y, Saito N, Endo M, Hasegawa Y *et al*. Effect of serum protein binding on real-time trafficking of liposomes with different charges analyzed by positron emission tomography. *Biochim Biophys Acta* 1996; **1280**: 149–154.
- Yoshida M, Takimoto R, Murase K, Sato Y, Hirakawa M, Tamura F *et al*. Targeting anticancer drug delivery to pancreatic cancer cells using a fucose-bound nanoparticle approach. *PLoS One* 2012; **7**: e39545.
- Hirai M, Minematsu H, Kondo N, Oie K, Igarashi K, Yamazaki N. Accumulation of liposome with Sialyl Lewis X to inflammation and tumor region: application to *in vivo* bio-imaging. *Biochem Biophys Res Commun* 2007; **353**: 553–558.
- Hirai M, Hiramatsu Y, Iwashita S, Otani T, Chen L, Li YG *et al*. E-selectin targeting to visualize tumors *in vivo*. *Contrast Media Mol Imaging* 2010; **5**: 70–77.
- French DC, Saltzgueber M, Hicks DR, Cowper AL, Holt DW. HPLC assay with ultraviolet detection for therapeutic drug monitoring of sirolimus. *Clin Chem* 2001; **47**: 1316–1319.
- Sapra P, Allen TM. Internalizing antibodies are necessary for improved therapeutic efficacy of antibody-targeted liposomal drugs. *Cancer Res* 2002; **62**: 7190–7194.
- Müller I, Jenner A, Bruchelt G, Niethammer D, Halliwell B. Effect of concentration on the cytotoxic mechanism of doxorubicin-apoptosis and oxidative DNA damage. *Biochem Biophys Res Commun* 1997; **230**: 254–257.
- Mukherjee T, Shah BV. Sirolimus: a new immunosuppressant. *J Assoc Physicians India*. 2005; **53**: 885–890.
- Nie Y, Ji L, Ding H, Xie L, Li L, He B *et al*. Cholesterol derivatives based charged liposomes for doxorubicin delivery: preparation, *in vitro* and *in vivo* characterization. *Theranostics* 2012; **2**: 1092–1103.
- Portell CA, Wenzell CM, Advani AS. Clinical and pharmacologic aspects of blinatumomab in the treatment of B-cell acute lymphoblastic leukemia. *Clin Pharmacol* 2013; **5**(Suppl 1): 5–11.



This work is licensed under a Creative Commons Attribution-NonCommercial-ShareAlike 3.0 Unported License. To view a copy of this license, visit <http://creativecommons.org/licenses/by-nc-sa/3.0/>

Supplementary Information accompanies this paper on Blood Cancer Journal website (<http://www.nature.com/bcj>)